

Article

## Efficient Synthesis of an Aluminum Amidoborane Ammoniate

Junzhi Yang <sup>1</sup>, Paul R. Beaumont <sup>2</sup>, Terry D. Humphries <sup>3</sup>, Craig M. Jensen <sup>2,\*</sup> and Xingguo Li <sup>1,\*</sup>

<sup>1</sup> Beijing National Laboratory for Molecular Sciences (BNLMS), the State Key Laboratory of Rare Earth Materials Chemistry and Applications, College of Chemistry and Molecular Engineering, Peking University, Beijing 100871, China; E-Mail: Jzyang@pku.edu.cn

<sup>2</sup> Department of Chemistry, University of Hawaii at Manoa, 2545 McCarthy Mall, Honolulu, HI 96822-2275, USA; E-Mail: p.r.beaumont@gmail.com

<sup>3</sup> Hydrogen Storage Research Group, Fuels and Energy Technology Institute, Department of Physics, Astronomy and Medical Radiation Sciences, Curtin University, GPO Box U1987, Perth, WA 6845, Australia; E-Mail: terry\_humphries81@hotmail.com

\* Authors to whom correspondence should be addressed;

E-Mails: Jensen@hawaii.edu (C.M.J.); xgli@pku.edu.cn (X.L.);

Tel./Fax: +1-808-956-2769 (C.M.J.); +86-10-6276-5930 (X.L.).

Academic Editor: Enrico Sciubba

Received: 6 July 2015 / Accepted: 6 August 2015 / Published: 26 August 2015

---

**Abstract:** A novel species of metal amidoborane ammoniate,  $[\text{Al}(\text{NH}_2\text{BH}_3)_6]^{3-}[\text{Al}(\text{NH}_3)_6]^{3+}$  has been successfully synthesized in up to 95% via the one-step reaction of  $\text{AlH}_3 \cdot \text{OEt}_2$  with liquid  $\text{NH}_3\text{BH}_3 \cdot n\text{NH}_3$  ( $n = 1\sim 6$ ) at 0 °C. This solution based reaction method provides an alternative pathway to the traditional mechano-chemical ball milling methods, avoiding possible decomposition. MAS  $^{27}\text{Al}$  NMR spectroscopy confirms the formulation of the compound as an  $\text{Al}(\text{NH}_2\text{BH}_3)_6^{3-}$  complex anion and an  $\text{Al}(\text{NH}_3)_6^{3+}$  cation. Initial dehydrogenation studies of this aluminum based M-N-B-H compound demonstrate that hydrogen is released at temperatures as low as 65 °C, totaling ~8.6 equivalents of  $\text{H}_2$  (10.3 wt %) upon heating to 105 °C. This method of synthesis offers a promising route towards the large scale production of metal amidoborane ammoniate moieties.

**Keywords:** aluminum; amidoborane; boranes; dehydrogenation; hydrogen storage; synthetic methods; Nuclear Magnetic Resonance Spectroscopy (NMR)

---

## 1. Introduction

A critical challenge facing the advancement of hydrogen fuel cells for automotive applications is the development of safe and energy efficient hydrogen storage materials. Metal amidoboranes ( $\text{MNH}_2\text{BH}_3$ , MAB) and metal borohydride ammoniates ( $\text{MBH}_4 \cdot n\text{NH}_3$ , MBA) are currently among the most promising candidate materials [1–6]. Recent demonstration of the regeneration of ammonia borane derivatives using hydrazine in liquid ammonia point to the feasibility of off-board reversibility [7–9]. Substitution of one protic H atom in the  $[\text{NH}_3]$  of  $\text{NH}_3\text{BH}_3$  by a metal atom leads to the formation of MAB complexes.

Aluminum amidoborane ( $\text{Al}(\text{NH}_2\text{BH}_3)_3$ , AlAB), first synthesized by Hawthorne *et al.* [10], possesses one of the highest theoretical hydrogen capacities among MABs (12.9 wt % H), capable of releasing 6 wt %  $\text{H}_2$  at 190 °C and approximately 8 wt %  $\text{H}_2$  in the presence of an ionic liquid at lower temperatures [10]. As such, this material has already experienced intensive explorations, although up to now only a few reports have identified its existence owing to its poor stability and spontaneous  $\text{H}_2$  loss caused by the chemically vulnerable Lewis-acidic  $\text{Al}^{3+}$  center [10–12]. The improved dehydrogenation properties of AlAB ( $\text{Al } \chi_p = 1.5$ ), relative to ammonia borane [10], makes the Al-N-B-H systems attractive, albeit difficult to synthesize. Recently, Guo *et al.* reported on the stability of  $[\text{Al}(\text{NH}_3)_6](\text{BH}_4)_3$  in air, which differs quite significantly from the analogous volatile liquid  $\text{Al}(\text{BH}_4)_3$  [13,14]. Strong  $\text{N-H}^{\delta+} \cdots \delta^- \text{H-B}$  dihydrogen bonds contribute to the stability of this compound resulting in its long term stability in air. Another recently reported Al based amidoborane complex includes  $\text{Li}_3\text{AlH}_6 \cdot n(\text{NH}_2\text{BH}_3)$  which releases 9 wt %  $\text{H}_2$  at a temperature of 130 °C [15].

A variety of B-N amidoborane ammoniates, have previously been synthesized by reacting MAB and  $\text{NH}_3$ , including  $\text{LiNH}_2\text{BH}_3 \cdot \text{NH}_3$  [16],  $\text{Mg}(\text{NH}_2\text{BH}_3)_2 \cdot 3\text{NH}_3$  [17], and  $\text{Ca}(\text{NH}_2\text{BH}_3)_2 \cdot \text{NH}_3$  [18]. However, to the best of our knowledge, there has been no prior report of the synthesis of an aluminum analog. Herein we report the first synthesis of aluminum amidoborane ammoniate,  $[\text{Al}(\text{NH}_2\text{BH}_3)_6]^{3-}[\text{Al}(\text{NH}_3)_6]^{3+}$ .

## 2. Results and Discussion

The synthesis of  $[\text{Al}(\text{NH}_2\text{BH}_3)_6]^{3-}[\text{Al}(\text{NH}_3)_6]^{3+}$  (according to Equations (1) and (2)) was achieved using a specially-designed polytetrafluoroethylene reactor, which allowed the reactants to be stirred at low temperature under ammonia pressure. Under these conditions, ammonia borane reversibly absorbs up to 6 equivalents of  $\text{NH}_3$ , forming liquid  $\text{NH}_3\text{BH}_3 \cdot n\text{NH}_3$  ( $n = 1-6$ ) complexes [19].  $\text{AlH}_3 \cdot \text{OEt}_2$ , which is insoluble in  $\text{NH}_3\text{BH}_3 \cdot n\text{NH}_3$ , was utilized as a highly reactive Al source [20,21]. Immersing the Al source in ammonia borane ammoniate complex permits the selective uptake of ammonia in a one-step synthesis of  $\text{Al}(\text{NH}_2\text{BH}_3)_3 \cdot 3\text{NH}_3$  as a solid precipitate that can be isolated in up to 95% purity (based on  $\text{AlH}_3 \cdot \text{OEt}_2$ ) by filtration (Equations (1) and (2), details in Section 3, Experimental Section). It should be emphasized that this method avoids the high-energy impact generally encountered in traditional ball milling methods and further prevents possible decomposition of components. This synthesis strategy may also be effective for other amidoborane ammoniates.

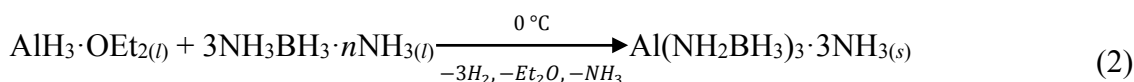
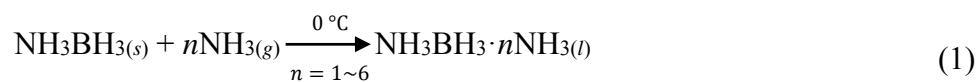
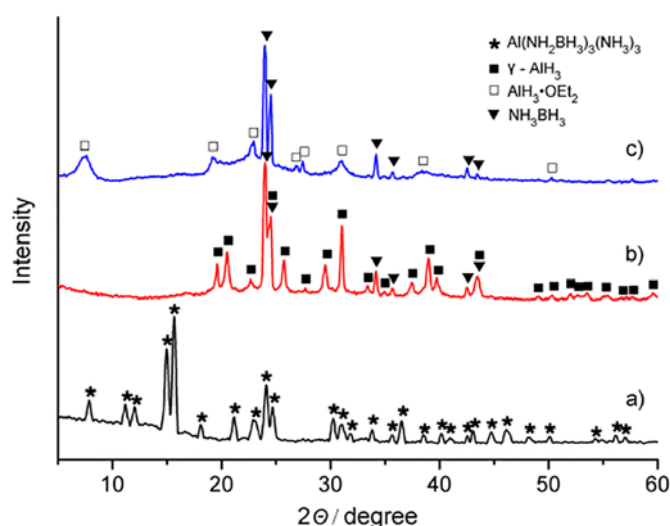
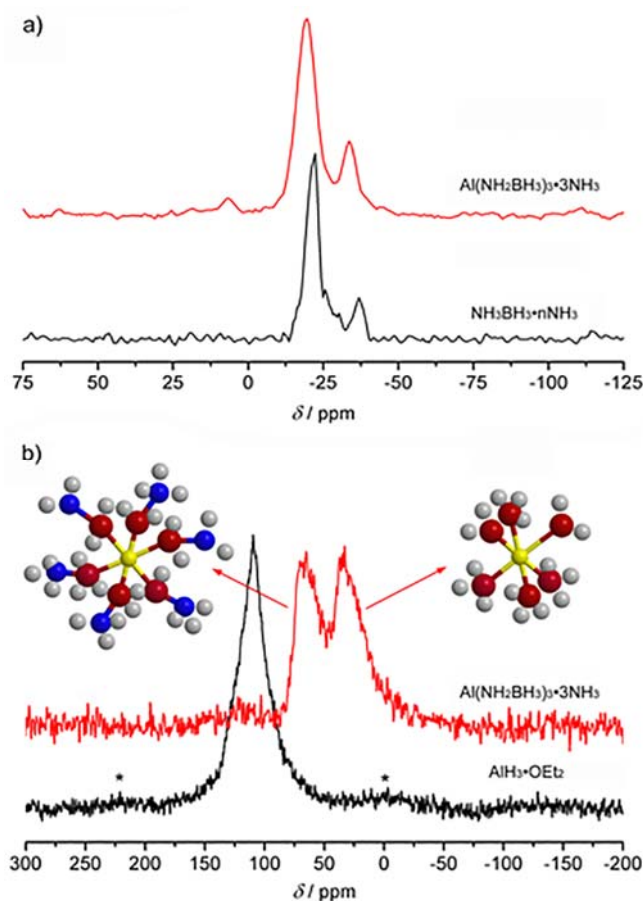


Figure 1a illustrates the XRD pattern obtained for a sample of  $\text{Al}(\text{NH}_2\text{BH}_3)_3 \cdot 3\text{NH}_3$  prepared via the method described above. The pattern does not index to any previously reported Al-N-B-H quaternary compound and contains at most, only very minor contributions from unreacted starting material. FTIR analysis of  $\text{Al}(\text{NH}_2\text{BH}_3)_3 \cdot 3\text{NH}_3$  featured a N-B stretch at  $875\text{ cm}^{-1}$  and peaks at  $426$  and  $461\text{ cm}^{-1}$  which were assigned to Al-N lattice vibrations, (Figure S1, Table S1). Attempts were also made to prepare  $\text{Al}(\text{NH}_2\text{BH}_3)_3 \cdot 3\text{NH}_3$  using ball milling techniques. As shown in Figure 1c, no new species evolved from a mixture of  $\text{AlH}_3 \cdot \text{OEt}_2 + 3\text{NH}_3\text{BH}_3$ , which was ball milled under ammonia atmosphere at  $0^\circ\text{C}$ , at a speed of 150 rpm for at least 2 hours. Moreover, increasing the ball milling energy, such as higher rotational speed or temperature ( $>40^\circ\text{C}$ ) during the synthesis causes dissociation of the ether adduct, which often leads to the production of  $\gamma\text{-AlH}_3$  (Figure 1b). This alane polymorph incidentally shows much lower reactivity in liquid  $\text{NH}_3\text{BH}_3 \cdot n\text{NH}_3$  than pure  $\text{AlH}_3 \cdot \text{OEt}_2$ , and inhibits the formation of an Al-N bond [22].



**Figure 1.** XRD patterns of (a) as-prepared  $\text{Al}(\text{NH}_2\text{BH}_3)_3 \cdot 3\text{NH}_3$ ; (b) mixture of  $\gamma\text{-AlH}_3 + 3\text{NH}_3\text{BH}_3$ ; (c) ball milled  $\text{AlH}_3 \cdot \text{OEt}_2 + 3\text{NH}_3\text{BH}_3$ .  $\lambda = 1.5406\text{ \AA}$ .

The  $^{27}\text{Al}$  MAS NMR spectrum (Figure 2b) verifies the formation of  $\text{Al}(\text{NH}_2\text{BH}_3)_3 \cdot 3\text{NH}_3$  and provides key information about its molecular structure. After reaction, only traces of the characteristic resonance for  $\text{AlH}_3 \cdot \text{OEt}_2$  at 109.9 ppm are observed [23]. Two major resonances at 65.5 ppm and 33.6 ppm dominate the spectrum, clearly indicating that  $\text{Al}(\text{NH}_2\text{BH}_3)_3 \cdot 3\text{NH}_3$  contains equal amounts of aluminum in two very different coordination environments. The MAS  $^{11}\text{B}$  NMR spectrum of the product contains a major resonance for  $\text{Al}(\text{NH}_2\text{BH}_3)_3 \cdot 3\text{NH}_3$  at 19.6 ppm and a minor resonance at  $-38$  ppm which is due to the presence of  $[(\text{NH}_3)_2\text{BH}_2^+][\text{BH}_4^-]$  DADB or a related decomposition product that was also observed in the starting material [24]. As seen in Figure 2a, the  $^{11}\text{B}$  chemical shift of  $\text{Al}(\text{NH}_2\text{BH}_3)_3 \cdot 3\text{NH}_3$  is 2.7 ppm upfield from the 22.3 ppm shift observed for  $\text{NH}_3\text{BH}_3 \cdot n\text{NH}_3$ . Similar upfield shifts have been observed for other metal amidoboranes and hence this observation confirms the substitution of an H atom by an Al atom in the ammonia borane molecule [25,26].



**Figure 2.** (a)  $^{11}\text{B}$  MAS NMR spectra of  $[\text{Al}(\text{NH}_2\text{BH}_3)_6]^{3-}[\text{Al}(\text{NH}_3)_6]^{3+}$  and  $\text{NH}_3\text{BH}_3 \cdot n\text{NH}_3$ ; (b)  $^{27}\text{Al}$  MAS NMR spectra of  $[\text{Al}(\text{NH}_2\text{BH}_3)_6]^{3-}[\text{Al}(\text{NH}_3)_6]^{3+}$  and  $\text{AlH}_3 \cdot \text{OEt}_2$ . The molecular structure of the octahedral Al complexes are also depicted (yellow balls represent Al, red for N, blue for B, and grey for H).

$\text{Al}^{3+}$  generally has either tetrahedral or octahedral coordination. Thus *a priori* there are four possible coordination geometries for  $\text{Al}(\text{NH}_2\text{BH}_3)_3 \cdot 3\text{NH}_3$ : 1) Al coordinates three  $(\text{NH}_2\text{BH}_3)^-$  anions and three ammonia molecules to give a neutral  $\text{Al}(\text{NH}_3)_3(\text{NH}_2\text{BH}_3)_3$  complex; 2) Al coordinates octahedrally with only ammonia giving a hexamminealuminum cation [27],  $\text{Al}(\text{NH}_3)_6^{3+}$  and leaving three free  $(\text{NH}_2\text{BH}_3)^-$  anions; 3) Al coordinates tetrahedrally with  $(\text{NH}_2\text{BH}_3)^-$  anions, forming an  $\text{Al}(\text{NH}_2\text{BH}_3)_4^-$  anion and three of these anions pair with one  $\text{Al}(\text{NH}_3)_6^{3+}$ ; and 4) Al octahedrally coordinates with  $(\text{NH}_2\text{BH}_3)^-$  anions giving a  $\text{Al}(\text{NH}_2\text{BH}_3)_6^{3-}$  complex anion and ion pairs with the  $\text{Al}(\text{NH}_3)_6^{3+}$  cation. The observation of two peaks with equal intensity in the  $^{27}\text{Al}$  MAS NMR spectrum is consistent with only the  $[\text{Al}(\text{NH}_2\text{BH}_3)_6]^{3-}[\text{Al}(\text{NH}_3)_6]^{3+}$  formulation and as such the  $^{27}\text{Al}$  NMR resonances are assigned as follows:  $\text{Al}(\text{NH}_2\text{BH}_3)_6^{3-}$  at 65.5 ppm and  $\text{Al}(\text{NH}_3)_6^{3+}$  at 33.6 ppm (Figure 2b). This is quite similar to the reported structure of  $\text{Mg}(\text{NH}_2\text{BH}_3)_2 \cdot 3\text{NH}_3$  where  $\text{Mg}^{2+}$  exhibits both tetrahedral and octahedral coordination [17]. Elemental analysis (Table S2) also shows the ratio of Al:N:B is 1:6:3, and supports the  $[\text{Al}(\text{NH}_2\text{BH}_3)_6]^{3-}[\text{Al}(\text{NH}_3)_6]^{3+}$  formulation.

No apparent reaction was observed after exposure of a sample of  $[\text{Al}(\text{NH}_2\text{BH}_3)_6]^{3-}[\text{Al}(\text{NH}_3)_6]^{3+}$  to dry air for 3 days (Figure S2). The time-programmed-desorption/mass spectroscopy (TPD/MS) results reveal that the thermal decomposition of  $[\text{Al}(\text{NH}_2\text{BH}_3)_6]^{3-}[\text{Al}(\text{NH}_3)_6]^{3+}$  occurs in the temperature range of

65–180 °C, with the release corresponding to 7.5 wt % (Figure 3a,c). The desorbed gaseous product comprises of both H<sub>2</sub> and NH<sub>3</sub>.

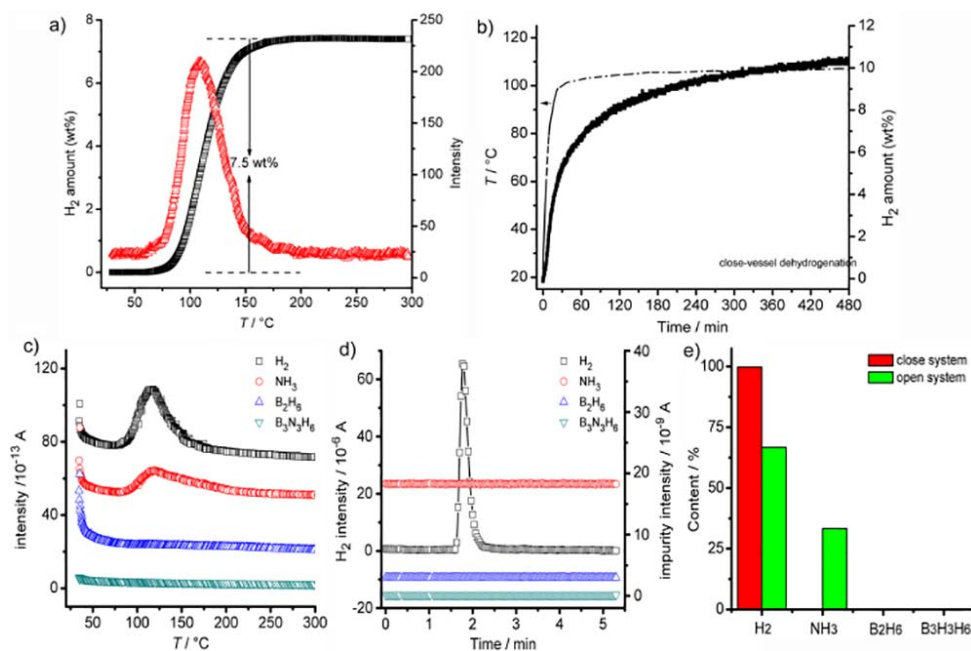


**Figure 3.** (a) TPD ( $\Delta$ ) and gas release ( $\square$ ) profiles of  $[\text{Al}(\text{NH}_2\text{BH}_3)_6^{3-}][\text{Al}(\text{NH}_3)_6^{3+}]$  at a heating rate of  $5\text{ }^\circ\text{C min}^{-1}$  under argon flow; (b) Isothermal desorption of  $[\text{Al}(\text{NH}_2\text{BH}_3)_6^{3-}][\text{Al}(\text{NH}_3)_6^{3+}]$  in a closed vessel; the temperature ramping shown by dash dot line; (c) MS signals in (a):  $\square$  H<sub>2</sub>,  $\circ$  NH<sub>3</sub>,  $\Delta$  B<sub>2</sub>H<sub>6</sub>,  $\nabla$  B<sub>3</sub>N<sub>3</sub>H<sub>6</sub>; (d) MS signals in (b) measured using Calibration Injection Mode:  $\square$  H<sub>2</sub>,  $\circ$  NH<sub>3</sub>,  $\Delta$  B<sub>2</sub>H<sub>6</sub>,  $\nabla$  B<sub>3</sub>N<sub>3</sub>H<sub>6</sub>; (e) H<sub>2</sub> purity comparison between different systems.

Figure 4 shows the N 1s XPS results of AlAB·3NH<sub>3</sub> before and after thermal decomposition (experimental details described in Supplemental Information). The peaks at  $\sim 396.6$ ,  $\sim 398.0$  and  $\sim 399.6$  eV are attributed to N-Al, N-B and NH<sub>3</sub>, respectively. After decomposition, the evolution of NH<sub>3</sub> and the corresponding peak at  $\sim 189.8$  eV in B 1s XPS (Figure S3) suggests the formation of an Al-N-B matrix. Combined with the remaining B-H vibrations in micro-FTIR (Figure S4, Table S3), the reaction under dynamic inert gas flow can be described by Equation (3). The anticipated borazine-derived structure is illustrated in Figure S5 representing AlN<sub>3</sub>B<sub>3</sub>H<sub>6</sub>.



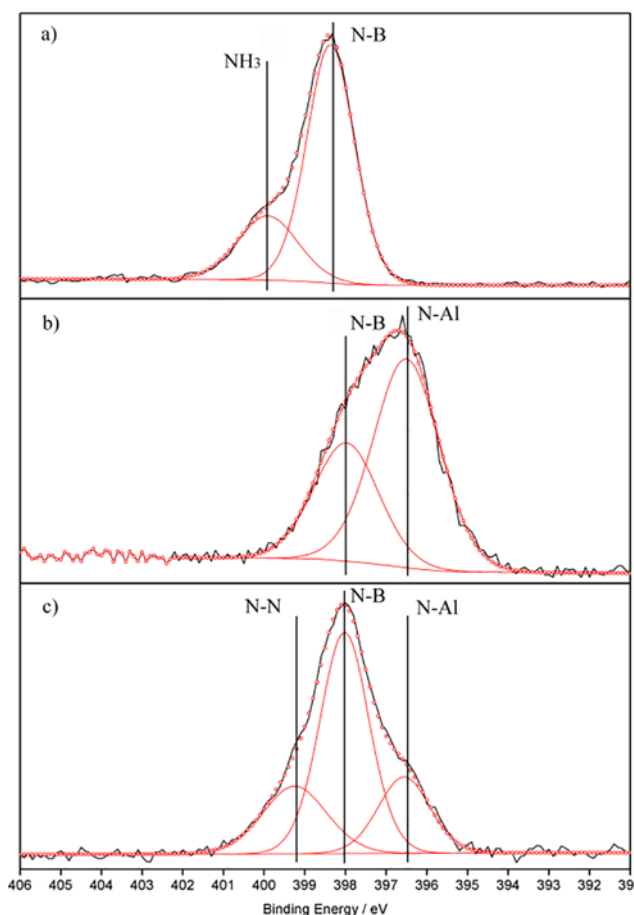


**Figure 4.** The N 1s XPS results of  $\text{Al}(\text{NH}_2\text{BH}_3)_3 \cdot 3\text{NH}_3$  (**1**) before (a) and after thermal decomposition in an open system (b) and in a closed system (c). The experiment data are in black, while the fitted ones are in red.

The isothermal desorption in a closed vessel was examined using a Sieverts method at 105 °C (experimental details described in Supplemental Information). The gas evolved is calculated to be 10.3 wt % (Figure 3b), while only 0.05%  $\text{NH}_3$  is detectable (Figure 3d). Obviously, the mass difference (Figure 3e) indicates that a significant partial pressure of  $\text{NH}_3$  in a closed system suppresses further  $\text{NH}_3$  desorption. This phenomenon is in accordance with the decomposition pathways of other metal amidoborane ammoniates [17,28,29]. Element analysis shows that the composition of Al, N, B and H are 15.83%, 48.18%, 18.36% and 3.83%, respectively, indicating an empirical formula of  $\text{AlN}_6\text{B}_3\text{H}_{6.5}^*$ . Similarly, N-H or B-H vibrations are not observed in the micro-FTIR spectrum, while Al-N stretching vibrations and weak H wagging vibrations are apparent (Figure S4 and Table S3). Meanwhile, the peaks at 1367 and 1627  $\text{cm}^{-1}$  are typical of N-B stretching in *h*-BN [30]. The N 1s XPS peak ~396.4 eV (Figure 4c) and is attributed to the formation of an Al-N bond, while the two overlapped B 1s XPS peaks in Figure S3 suggests that the decomposed product comprises of not only  $[\text{AlNBH}]$  but also another B moiety. On the other hand, the  $^{11}\text{B}$  MAS NMR spectrum presents at least two overlapping resonances at 6.3 ppm and 18.3 ppm (Figure S6), which is due to the second-order quadrupolar interaction. Thus, the B atoms are likely in a  $\text{BN}_3$  or  $\text{BN}_2\text{H}$  environment [31,32]. The N 1s peak at ~399.1 eV is possibly a N-N bond. Clearly, the decomposition mechanism of  $[\text{Al}(\text{NH}_2\text{BH}_3)_6]^{3-}[\text{Al}(\text{NH}_3)_6]^{3+}$  in a closed system is

much more complicated than that of an open system. On the basis of 8.6 equivalents of H<sub>2</sub>, the dehydrogenation process can be briefly described by Equation (4).



### 3. Experimental Section

All starting materials, LiAlH<sub>4</sub> 99% (Sigma-Aldrich, Shanghai, China), AlCl<sub>3</sub> 99.99%, NH<sub>3</sub>BH<sub>3</sub> 99% (Sigma-Aldrich), and NH<sub>3</sub> (Alfa Aesar, Shanghai, China), were obtained commercially and used without further purification. All manipulations were carried out under inert atmosphere conditions, either in an argon-filled glovebox or using standard Schlenk line techniques under a nitrogen atmosphere. The organometallic synthesis of AlH<sub>3</sub>·Et<sub>2</sub>O is a chemically simple process, but a brief summary is presented. Generally, AlCl<sub>3</sub> was reacted with LiAlH<sub>4</sub> in diethyl ether with the LiCl precipitate being removed by filtration [21,33]. The excess diethyl ether was then removed under dynamic vacuum. AlH<sub>3</sub>·Et<sub>2</sub>O was ground in a mortar with excess NH<sub>3</sub>BH<sub>3</sub> and then sealed in a self-designed polytetrafluoroethylene (PTFE) reactor. The reactor was attached to the gas/vacuum manifold and rapidly evacuated/backfilled with 0.3–0.5 MPa NH<sub>3</sub>. The system was cooled to –70 °C using acetone and dry ice, and gradually warmed to 0 °C in an ice bath. At this temperature and under the NH<sub>3</sub> atmosphere, ammonia borane reversibly absorbed up to at least 6 equivalents of NH<sub>3</sub>, forming liquid NH<sub>3</sub>BH<sub>3</sub>·*n*NH<sub>3</sub> (*n* = 1–6) complexes. AlH<sub>3</sub>·OEt<sub>2</sub> was dissolved in liquid NH<sub>3</sub>BH<sub>3</sub>·*n*NH<sub>3</sub>, and the solution stirred for 2 h until the reaction was complete. The internal temperature and pressure of the reactor and manifold were recorded for the duration of the experiment. The ammonia and reaction produced hydrogen were then removed *in vacuo* at room temperature. Anhydrous diethyl ether was then added to the remaining products, thereby dissolving the excess NH<sub>3</sub>BH<sub>3</sub> of which was removed by filtration. The residual solid [Al(NH<sub>2</sub>BH<sub>3</sub>)<sub>6</sub><sup>3-</sup>][Al(NH<sub>3</sub>)<sub>6</sub><sup>3+</sup>] was then heated to 45 °C for 12h to remove residual solvent to yield a solid white powder.

### 4. Conclusions

In summary, a novel aluminum amidoborane ammoniate, [Al(NH<sub>2</sub>BH<sub>3</sub>)<sub>6</sub><sup>3-</sup>][Al(NH<sub>3</sub>)<sub>6</sub><sup>3+</sup>], has been successfully synthesized. A reaction vessel has been designed that allows a one-step synthesis from the reaction of AlH<sub>3</sub>·OEt<sub>2</sub> with liquid NH<sub>3</sub>BH<sub>3</sub>·*n*NH<sub>3</sub> (*n* = 1–6) at 0 °C. MAS <sup>27</sup>Al NMR spectroscopy confirms the formulation of the compound as an Al(NH<sub>2</sub>BH<sub>3</sub>)<sub>6</sub><sup>3-</sup> complex anion and a Al(NH<sub>3</sub>)<sub>6</sub><sup>3+</sup> cation. This aluminum based M-N-B-H compound begins to release hydrogen at 65 °C, amounting to ~8.6 equivalents of H<sub>2</sub> (10.3 wt %) upon heating to 105 °C. This method of synthesis offers a promising route towards the large scale production of metal amidoborane ammoniate moieties.

### Supplementary Materials

Supplementary materials can be accessed at: <http://www.mdpi.com/1996-1073/8/9/9107/s1>.

### Acknowledgments

The authors would like to acknowledge the financial support given by the MOST of China (No. 2010CB631301, 2009CB939902 and 2012CBA01207) and the NSFC (No. U1201241 and 51071003).

## Conflicts of Interest

The authors declare no conflict of interest.

## References

1. Staubitz, A.; Robertson, A.P.M.; Manners, I. Ammonia-borane and related compounds as dihydrogen sources. *Chem. Rev.* **2010**, *110*, 4079–4124.
2. Chua, Y.S.; Chen, P.; Wu, G.; Xiong, Z. Development of amidoboranes for hydrogen storage. *Chem. Commun.* **2011**, *47*, 5116–5129.
3. Zhang, Y.S.; Wolverton, C. Crystal structures, phase stabilities, and hydrogen storage properties of metal amidoboranes. *J. Phys. Chem. C* **2012**, *116*, 14224–14231.
4. Zheng, X.L.; Wu, G.T.; Li, W.; Xiong, Z.T.; He, T.; Guo, J.P.; Chen, H.; Chen, P. Releasing 17.8 wt% H<sub>2</sub> from lithium borohydride ammoniate. *Energy Environ. Sci.* **2011**, *4*, 3593–3600.
5. Guo, Y.H.; Wu, H.; Zhou, W.; Yu, X.B. Dehydrogenation tuning of ammine borohydrides using double-metal cations. *J. Am. Chem. Soc.* **2011**, *133*, 4690–4693.
6. Jepsen, L.H.; Ley, M.B.; Lee, Y.-S.; Cho, Y.W.; Dornheim, M.; Jensen, J.O.; Filinchuk, Y.; Jørgensen, J.E.; Besenbacher, F.; Jensen, T.R.; *et al.* Boron-nitrogen based hydrides and reactive composites for hydrogen storage. *Mater. Today* **2014**, *17*, 129–135.
7. Sutton, A.D.; Burrell, A.K.; Dixon, D.A.; Garner, E.B.; Gordon, J.C.; Nakagawa, T.; Ott, K.C.; Robinson, P.; Vasiliu, M. Regeneration of ammonia borane spent fuel by direct reaction with hydrazine and liquid ammonia. *Science* **2011**, *331*, 1426–1429.
8. Tang, Z.W.; Tan, Y.B.; Chen, X.W.; Yu, X.B. Regenerable hydrogen storage in lithium amidoborane. *Chem. Commun.* **2012**, *48*, 9296–9298.
9. Li, S.; Tang, Z.; Gong, Q.; Yu, X.; Beaumont, P.R.; Jensen, C.M. Phenyl introduced ammonium borohydride: Synthesis and reversible dehydrogenation properties. *J. Mater. Chem.* **2012**, *22*, 21017–21023.
10. Hawthorne, M.F.; Jalisatgi, S.S.; Safronov, A.V.; Lee, H.B.; Wu, J. Chemical Hydrogen Storage Using Polyhedral Borane Anions and Aluminum-Ammonia-Borane Complexes. Available online: <http://www.osti.gov/scitech//servlets/purl/990217-xUxbgx/> (accessed on 28 June 2015).
11. Harder, S.; Spielmann, J. Unprecedented reactivity of an aluminium hydride complex with ArNH<sub>2</sub>BH<sub>3</sub>: Nucleophilic substitution *versus* deprotonation. *Chem. Commun.* **2011**, *47*, 11945–11947.
12. Dou, D.; Ketchum, D.R.; Hamilton, E.J.M.; Florian, P.A.; Vermillion, K.E.; Grandinetti, P.J.; Shore, S.G. Reactions of aluminum hydride derivatives with ammonia-borane: A new approach toward AlN/BN materials. *Chem. Mater.* **1996**, *8*, 2839–2842.
13. Guo, Y.; Yu, X.; Sun, W.; Sun, D.; Yang, W. The hydrogen-enriched Al-B-N system as an advanced solid hydrogen-storage candidate. *Angew. Chem. Int. Ed.* **2011**, *50*, 1087–1091.
14. Guo, Y.H.; Jiang, Y.X.; Xia, G.L.; Yu, X.B. Ammine aluminium borohydrides: An appealing system releasing over 12 wt% pure H<sub>2</sub> under moderate temperature. *Chem. Commun.* **2012**, *48*, 4408–4410.
15. Xia, G.; Tan, Y.; Chen, X.; Guo, Z.; Liu, H.; Yu, X. Mixed-metal (Li, Al) amidoborane: Synthesis and enhanced hydrogen storage properties. *J. Mater. Chem. A* **2013**, *1*, 1810–1820.



16. Xia, G.L.; Yu, X.B.; Guo, Y.H.; Wu, Z.; Yang, C.Z.; Liu, H.K.; Dou, S.X. Ammine lithium amidoborane  $\text{Li}(\text{NH}_3)\text{NH}_2\text{BH}_3$ : A new coordination compound with favorable dehydrogenation characteristics. *Chem. Eur. J.* **2010**, *16*, 3763–3769.
17. Kang, X.D.; Wu, H.; Luo, J.H.; Zhou, W.; Wang, P. A simple and efficient approach to synthesize amidoborane ammoniates: Case study for  $\text{Mg}(\text{NH}_2\text{BH}_3)_2(\text{NH}_3)_3$  with unusual coordination structure. *J. Mater. Chem.* **2012**, *22*, 13174–13179.
18. Chua, Y.S.; Wu, H.; Zhou, W.; Udovic, T.J.; Wu, G.T.; Xiong, Z.T.; Wong, M.W.; Chen, P. Monoammoniate of calcium amidoborane: Synthesis, structure, and hydrogen-storage properties. *Inorg. Chem.* **2012**, *51*, 1599–1603.
19. Gao, L.; Fang, H.C.; Li, Z.H.; Yu, X.B.; Fan, K.N. Liquefaction of solid-state  $\text{BH}_3\text{NH}_3$  by gaseous  $\text{NH}_3$ . *Inorg. Chem.* **2011**, *50*, 4301–4306.
20. Graetz, J.; Chaudhuri, S.; Wegrzyn, J.; Celebi, Y.; Johnson, J.R.; Zhou, W.; Reilly, J.J. Direct and reversible synthesis of  $\text{AlH}_3$ -triethylenediamine from Al and  $\text{H}_2$ . *J. Phys. Chem. C* **2007**, *111*, 19148–19152.
21. Brower, F.M.; Matzek, N.E.; Reigler, P.F.; Rinn, H.W.; Roberts, C.B.; Schmidt, D.L.; Snover, J.A.; Terada, K. Preparation and properties of aluminum-hydride. *J. Am. Chem. Soc.* **1976**, *98*, 2450–2453.
22. Giannasi, A.; Colognesi, D.; Fichtner, M.; Rohm, E.; Ulivi, L.; Ziparo, C.; Zoppi, M. Temperature behavior of the  $\text{AlH}_3$  polymorph by *in situ* investigation using high resolution raman scattering. *J. Phys. Chem. A* **2011**, *115*, 691–699.
23. Humphries, T.D.; Munroe, K.T.; Decken, A.; McGrady, G.S. Lewis base complexes of  $\text{AlH}_3$ : Prediction of preferred structure and stoichiometry. *Dalton Trans.* **2013**, *42*, 6965–6978.
24. Stowe, A.C.; Shaw, W.J.; Linehan, J.C.; Schmid, B.; Autrey, T. *In situ* solid state  $^{11}\text{B}$  MAS-NMR studies of the thermal decomposition of ammonia borane: Mechanistic studies of the hydrogen release pathways from a solid state hydrogen storage material. *Phys. Chem. Chem. Phys.* **2007**, *9*, 1831–1836.
25. Shimoda, K.; Zhang, Y.; Ichikawa, T.; Miyaoka, H.; Kojima, Y. Solid state NMR study on the thermal decomposition pathway of sodium amidoborane  $\text{NaNH}_2\text{BH}_3$ . *J. Mater. Chem.* **2011**, *21*, 2609–2615.
26. Shimoda, K.; Doi, K.; Nakagawa, T.; Zhan, Y.; Miyaoka, H.; Ichikawa, T.; Tansho, M.; Shimizu, T.; Burrell, A.K.; Kojima, Y. Comparative study of structural changes in  $\text{NH}_3\text{BH}_3$ ,  $\text{LiNH}_2\text{BH}_3$ , and  $\text{KNH}_2\text{BH}_3$  during dehydrogenation process. *J. Phys. Chem. C* **2012**, *116*, 5957–5964.
27. Semenenko, K.N.; Shilkin, S.P.; Polyakova, V.B. Vibrational spectra and structure of the di- and tetraammoniate of aluminum borohydride. *Bull. Acad. Sci. USSR Div. Chem. Sc.* **1978**, *27*, 859–864.
28. Chua, Y.S.; Wu, G.T.; Xiong, Z.T.; Karkamkar, A.; Guo, J.P.; Jian, M.X.; Wong, M.W.; Autrey, T.; Chen, P. Synthesis, structure and dehydrogenation of magnesium amidoborane monoammoniate. *Chem. Commun.* **2010**, *46*, 5752–5754.
29. Chua, Y.S.; Wu, G.T.; Xiong, Z.T.; He, T.; Chen, P. Calcium amidoborane ammoniate-synthesis, structure, and hydrogen storage properties. *Chem. Mater.* **2009**, *21*, 4899–4904.
30. Geick, R.; Perry, C.; Rupprecht, G. Normal modes in hexagonal boron nitride. *Phys. Rev.* **1966**, *146*, 543–547.

31. Marchetti, P.S.; Kwon, D.K.; Schmidt, W.R.; Interrante, L.V.; Maciel, G.E. High-field B11 magic angle spinning NMR characterization of boron nitrides. *Chem. Mater.* **1991**, *3*, 482–486.
32. Jeschke, G.; Hoffbauer, W.; Jansen, M. A comprehensive NMR study of cubic and hexagonal boron nitride. *Solid State Nucl. Magn. Reson.* **1998**, *12*, 1–7.
33. Humphries, T.D.; Munroe, K.T.; DeWinter, T.M.; Jensen, C.M.; McGrady, G.S. NMR spectroscopic and thermodynamic studies of the etherate and the  $\alpha$ ,  $\alpha'$ , and  $\gamma$  phases of  $\text{AlH}_3$ . *Int. J. Hydrog. Energy* **2013**, *38*, 4577–4586.

© 2015 by the authors; licensee MDPI, Basel, Switzerland. This article is an open access article distributed under the terms and conditions of the Creative Commons Attribution license (<http://creativecommons.org/licenses/by/4.0/>).